Grasping and In-Hand Manipulation: Geometry and Algorithms

Attawith Sudsang, Jean Ponce and Narayan Srinivasa
Beckman Institute, University of Illinois, Urbana, IL 61801

Abstract

This paper addresses the problem of grasping and manipulating three-dimensional objects with a reconfigurable gripper that consists of two parallel plates whose distance can be adjusted by a computer-controlled actuator. The bottom plate is a bare plane, and the top plate carries a rectangular grid of actuated pins that can translate in discrete increments under computer control. We propose to use this gripper to immobilize objects through frictionless contacts with three of the pins and the bottom plate, and to manipulate an object within a grasp by planning the sequence of pin configurations that will bring this object to a desired position and orientation. A detailed analysis of the problem geometry in configuration space is used to devise simple and efficient algorithms for grasp and manipulation planning. The proposed approach has been implemented and preliminary simulation experiments are discussed.

1   Introduction

Classical parallel-jaw grippers are unable to adapt to a wide variety of workpiece geometries; although dextrous hands have been proposed by the academic robotics community [19, 47], they are too expensive and cumbersome for typical manufacturing applications. Thus different grippers are used for different parts (hundreds of different models are indeed listed by gripper manufacturers). This calls for the design of reconfigurable grippers which combine the flexibility of dextrous hands with the cost-effectiveness and simplicity of parallel-jaw grippers, and for the development of accompanying software to reconfigure these grippers according to part geometry.

We address in this article the problem of grasping and manipulating three-dimensional polyhedral objects using a new reconfigurable gripper, currently under construction at the University of Illinois [35, 49]. The gripper consists of two parallel plates whose distance can be adjusted by a computer-controlled actuator (Figure 1). The bottom plate is a bare plane, and the top plate carries a rectangular grid of actuated pins that can translate in discrete increments under computer control.

We propose to use this gripper to immobilize objects through frictionless contacts with three of the pins and the bottom plate, and to manipulate an object within a grasp by planning the sequence of pin configurations that will bring this object to a desired position and orientation.

Our approach is based on the notion of second-order immobility introduced by Rimon and Burdick [43] and on a detailed analysis of the geometry of the joint object/gripper configuration space. Characterizing the range of possible object motions associated with a grasp configuration allows us to identify the "minimal" configurations for which the object is totally immobilized as well as the "maximal" ones for which there is a non-empty open set of object motions within the grasp, but no escape path to infinity.
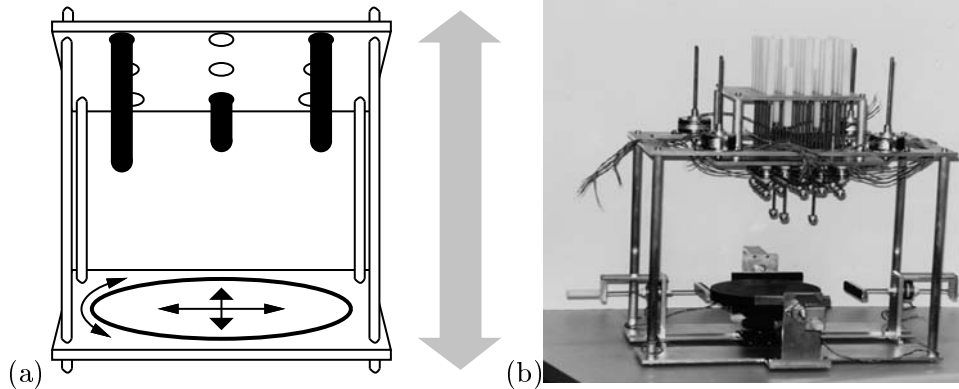
Figure 1: A reconfigurable gripper: (a) conceptual design and (b) actual prototype. To simulate the absence of friction, the bottom plate is mounted on three low-friction translational and rotational stages. This is reminiscent of Goldberg's sliding-jaw gripper [15].

The minimal configurations are the basis for grasping, and the maximal ones are the basis for in-hand manipulation. In addition, our analysis decouples the continuous and discrete degrees of freedom of the gripper, which allows us to devise efficient algorithms for grasp and manipulation planning. We have implemented the proposed approach and present preliminary simulation experiments.

1.1 Related Work

When a hand holds an object at rest, the forces and moments exerted by the fingers should balance each other so as not to disturb the position of this object. We say that such a grasp achieves *equilibrium*. For the hand to hold the object securely, it should also be capable of preventing any motion due to external forces and torques. Since screw theory [2, 18, 33] can be used to represented both displacements (*twists*) and forces and moments (*wrenches*), it is an appropriate tool for analyzing and synthesizing grasps. Indeed, it is known that six independent contact wrenches are necessary to prevent any infinitesimal displacement which maintains contact, and that a seventh one is required to ensure that contact cannot be broken [20, 48]. Such a grasp prevents any infinitesimal motion of the object, and it is said to achieve *form closure* [33, 41, 47]. A system of wrenches is said to achieve *force closure* when it can balance any external force and torque. Like wrenches and infinitesimal twists [46], force and form closure are dual notions and, as noted in [30, 31] for example, force closure implies form closure and vice versa.

The notions of form and force closure are the traditional theoretical basis for grasp planning algorithms. Mishra, Schwartz, and Sharir [29] have proposed linear-time algorithms for computing a finger configuration achieving force closure for frictionless polyhedral objects. Markenscoff and Papadimitriou [25] and Mirtich and Canny [27] have proposed algorithms for planning grasps which are optimal according to various criteria [13]. In each of these works, the grasp-planning algorithm outputs a single grasp for a given set of contact faces. Assuming Coulomb friction [31], Nguyen has proposed instead a geometric method for computing *maximal independent* two-finger grasps of polygons, i.e., segments of the polygonal boundary where the two fingers can be positioned independently while maintaining force closure, requiring as little positional accuracy from the robot as possible. This approach has been generalized to handle various numbers of fingers and different object geometries in [3, 8, 34, 36, 37, 38]

2

Robotic grasping and fixture planning are related problems (in both cases, the object grasped of fixtured must, after all, be held securely), but their functional requirements are not the same: as remarked by Chou, Chandru, and Barash [9], machining a part requires much better positional accuracy than simply picking it up, and the range of forces exerted on the parts are very different. The role of friction forces is also different: in the grasping context, where fingers are often covered with rubber or other soft materials, friction effects can be used to lower the number of fingers required to achieve form closure from seven to four; in the fixturing context, on the other hand, it is customary to assume frictionless contact, partly due to the large magnitude and inherent dynamic nature of the forces involved [9] (see, however [23] for an approach to fixture planning with friction). Finally, the kinematic constraints on the positions of the contacts are also quite different: in particular, dextrous grippers have *continuous* degrees of freedom, corresponding to the various finger joints, while modular fixtures have mostly *discrete* degrees of freedom, corresponding for example to the position of pins on an integer grid attached to a fixturing plate.

As noted by Wallack [52], there has recently been a renewed interest in the academic robotics community for manufacturing problems in general and fixturing in particular. Mishra has studied the problem of designing fixtures for rectilinear parts using toe clamps attached to a regular grid, and proven the existence of fixtures using six clamps [28] (this result has since then been tightened to four clamps by Zhuang, Goldberg, and Wong [53]). In keeping with the idea of *Reduced Intricacy Sensing and Control (RISC)* robotics of Canny and Goldberg [6], Wallack and Canny [51, 52] and Brost and Goldberg [4] have recently proposed very simple modular fixturing devices and efficient algorithms for constructing form-closure fixtures of two-dimensional polygonal and curved objects. Brost and Peters [5] have extended this approach to prismatic three-dimensional objects, and Wagner, Zhuang, and Goldberg [50] have proposed a three-dimensional seven-contact fixturing device and an algorithm for planning form-closure fixtures of a polyhedron with pre-specified pose.

Recently, Rimon and Burdick have introduced the notion of *second-order immobility* [43, 44, 45] and shown that certain equilibrium grasps (or fixtures) of a part which do not achieve form closure effectively prevent any *finite* motion of this part through curvature effects in configuration space. They have given operational conditions for immobilization and proven the dynamic stability of immobilizing grasps under various deformation models [45]. An additional advantage of their theory is that second-order immobilization can be achieved with fewer fingers (four contacts for convex fingers) than form closure (seven contacts [20, 48]).

In [35, 49], we introduced a new approach to modular fixture planning, based on the notion of second-order immobility. We proposed to bridge the gap between fixture and grasp planning by considering a new class of reconfigurable grippers with mostly discrete degrees of freedom, which have the potential of achieving the same level of flexibility as dextrous robotic hands for a fraction of the cost. We also gave an algorithm for grasp planning and reported preliminary results. In this paper, we improve the grasp planning algorithm of [35, 49] and introduce a new approach to in-hand manipulation. This approach is related to a number of sensorless pushing and squeezing manipulation algorithms [1, 12, 16, 24, 26, 40, 42], and it is based on an explicit configuration space characterization of the possible range of motions of the manipulated part as contact occurs.

1.2   Second-Order Immobility

Let us consider a rigid object and the contacts between d pins and this object. We assume frictionless hard-finger contacts, so each pin exerts a pure force on the grasped object at the point of contact. The force $\boldsymbol{f}$ exerted at the point $\boldsymbol{p}$ and its moment can be represented by the *zero-pitch*

wrench [2, 18, 33]

$$\boldsymbol{w} = \begin{pmatrix} \boldsymbol{f} \\ \boldsymbol{p} \times \boldsymbol{f} \end{pmatrix},$$

where "$\times$" denotes the operator that associates to two vectors their cross-product.

Let us denote by $\boldsymbol{p}_i$ $(i = 1, .., d)$ the positions of the contacts in a coordinate frame attached to the object, and by $\boldsymbol{n}_i$ $(i = 1, .., d)$ the unit inward normals to the corresponding faces. Equilibrium is achieved when the contact wrenches balance each other, i.e.,

$$\sum_{i=1}^{d} \lambda_i \begin{pmatrix} \boldsymbol{n}_i \\ \boldsymbol{p}_i \times \boldsymbol{n}_i \end{pmatrix} = 0, \tag{1}$$

for some $\lambda_i \geq 0$ $(i = 1, .., d)$ with $\sum_{i=1}^{d} \lambda_i = 1$ (note that the value of a wrench depends on the choice of origin, but that the condition for equilibrium does not). Equilibrium is a necessary, but not sufficient, condition for force and form closure.

Czyzowicz, Stojmenovic and Urrutia have recently shown that three contacts in the plane and four contacts in the three-dimensional case are sufficient to immobilize (i.e., prevent any *finite* motion of) a polyhedron [10]. Rimon and Burdick have formalized the notion of immobilizing grasps and fixtures in terms of isolated points of the free configuration space [43, 44, 45] (see also related work by Mirtich and Canny [27]). They have shown that equilibrium fixtures that do not achieve form closure may still immobilize an object through second-order (curvature) effects in configuration space: a sufficient condition for immobility is that the *relative curvature form* associated with an essential equilibrium grasp or fixture be negative definite (essential equilibrium is achieved when the coefficients λ_i in (1) are uniquely defined and strictly positive[44]). The relative curvature form can be computed in terms of the contact positions as well as the surface normals and curvatures of the body and pins at the contacts.

In the case of equilibrium contacts between pins with a spherical tip and polyhedra, it is easily shown [35] that the symmetric matrix associated with the relative curvature form is

$$\mathcal{K} = \sum_{i=1}^{d} \lambda_i \{([\boldsymbol{n}_{i\times}]^T [\boldsymbol{p}_{i\times}])^S - r_i [\boldsymbol{n}_{i\times}]^T [\boldsymbol{n}_{i\times}]\}, \tag{2}$$

where r_i denotes the pin's radius, the weights λ_i are the equilibrium weights of (1), and, by definition, $\mathcal{A}^S = \frac{1}{2}(\mathcal{A} + \mathcal{A}^T)$.

Given an object/gripper equilibrium configuration, we can thus test whether the gripper will immobilize the object that it holds by computing the matrix $\mathcal{K}$ and checking whether it is negative definite. Note again that Rimon's and Burdick's condition is only sufficient for immobility, so an object failing this test may be immobilized due to third- or higher-order effects.

In grasping applications, *stability* is often as important as immobility: a part is said to be in stable equilibrium if it returns to its equilibrium position after having been subjected to a small displacement. Stability is very important in real mechanical systems which cannot be expected to have perfect accuracy. Nguyen has shown that force (or form) closure implies stability [32], but Donoghue, Howard and Kumar have shown that there exist stable grasps or fixtures which do not achieve form closure [11, 17]. Rimon and Burdick have proven the dynamic stability of second-order immobilizing grasps under various deformation models [45]. Thus we can be confident that a planned immobilizing grasp can successfully be executed even in the presence of small unknown object displacements. As shown in Section 3, it is in fact possible to characterize the set of *finite* displacements that a part may undergo without compromising a successful grasping operation. This will be the basis for the in-hand manipulation technique presented in that section.

2 Grasp Planning

We address the problem of grasping a three-dimensional polyhedral object with the reconfigurable gripper shown in Figure 1. We derive geometric conditions for contact, equilibrium, and immobility. We then use these conditions in a simple and efficient algorithm for enumerating all immobilizing grasps of a polyhedral object.

2.1 Geometry of the Problem

Our gripper can be used to hold a polyhedral object through contacts with three of the top plate pins, and either a face, an edge-and-vertex, or a three-vertex contact with the bottom plate. Let us assume for the sake of simplicity that the faces of the polyhedron are convex (note that we do not assume that the polyhedron itself is convex). Any wrench exerted at a contact point between a face and the bottom plate can be written as a positive combination of wrenches at the vertices. Likewise, the wrenches corresponding to an edge-and-vertex contact are positive combinations of wrenches exerted at the end-points of the line segment and at the vertex.

We detail the case of a contact between the bottom plate and a triangular face f with inward unit normal $\boldsymbol{n}$ and vertices $\boldsymbol{v}_i$ $(i = 1, 2, 3)$ and denote by f_i $(i = 1, 2, 3)$ the remaining faces, with inward unit normals $\boldsymbol{n}_i$ (Figure 2). We assume that f is triangular for technical reasons that will become clear in Section 2.1.2. As will be shown in Section 3, our approach can in fact handle arbitrary convex polygons, but this requires the finer geometric analysis presented in that section.
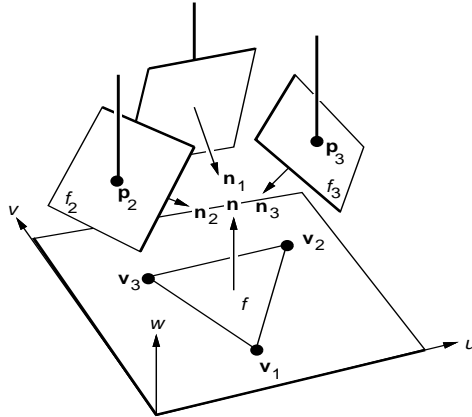
Figure 2: The four faces involved in a grasp.

We also assume without loss of generality that the four vectors $\boldsymbol{n}$ and $\boldsymbol{n}_i$ $(i = 1, 2, 3)$ *positively span* $\mathbb{R}^3$, i.e., that a strictly positive linear combination of these vectors is equal to zero (this is a necessary condition for essential equilibrium). Finally, given the physical layout of our gripper, contact between the upper-jaw pins and faces such that $\boldsymbol{n} \cdot \boldsymbol{n}_i > 0$ is of course impossible, and we further assume without loss of generality that $\boldsymbol{n} \cdot \boldsymbol{n}_i < 0$ for $i = 1, 2, 3$.

Under these assumptions, we can choose a coordinate system (u, v, w) attached to the object with w axis parallel to $\boldsymbol{n}$, and write in this coordinate system

$$\boldsymbol{n} = \begin{pmatrix} 0 \\ 0 \\ 1 \end{pmatrix} \quad \text{and} \quad \boldsymbol{n}_i = \frac{1}{l_i} \begin{pmatrix} a_i \\ b_i \\ -1 \end{pmatrix}, \quad \text{where} \quad l_i = \sqrt{1 + a_i^2 + b_i^2}.$$

Likewise, since the vectors $\boldsymbol{n}$ and $\boldsymbol{n}_i$ $(i = 1, 2, 3)$ positively span $\mathbb{R}^3$, we can write $\boldsymbol{n} = -\sum_{i=1}^3 \mu_i \boldsymbol{n}_i$, where $\mu_i > 0$ for $i = 1, 2, 3$. To complete the specification of the faces f_i $(i = 1, 2, 3)$,

we will denote by c_i the height of f_i at the origin, so the plane of this face can be parameterized by $w_i = a_i u_i + b_i v_i + c_i$. Finally, since the faces f_i are convex, we will express the fact that the point associated with the parameters u_i, v_i actually belongs to f_i by linear inequalities on u_i, v_i:

$$a_{ij} u_i + b_{ij} v_i + c_{ij} \leq 0, \quad j = 1, .., k_i, \tag{3}$$

where k_i is the number of edges bounding f_i.

2.1.1 Contact

We reduce the problem of achieving contact between a spherical pin and a plane to the problem of achieving point contact with a plane. This is done without loss of generality by growing the object to be fixtured by the pin radius and shrinking the spherical end of the pin into its center (see [6, 51, 52] for a similar approach in the two-dimensional case). We attach a coordinate system (q, r, w) to the gripper, and denote by $\mathcal{R}$ and $\boldsymbol{t}$ the rotation of angle θ about $\boldsymbol{n}$ and the translation (x, y) in the plane orthogonal to $\boldsymbol{n}$ that map the (q, r, w) coordinate system onto the (u, v, w) coordinate system.

If $\boldsymbol{p}_i$ and $\boldsymbol{q}_i$ denote respectively the positions of the tip of pin number i in the object's and gripper's coordinate frames, we can write

$$\boldsymbol{p}_i = \begin{pmatrix} u_i \\ v_i \\ a_i u_i + b_i v_i + c_i \end{pmatrix}, \quad \boldsymbol{q}_i = \begin{pmatrix} q_i \\ r_i \\ \delta - h_i \end{pmatrix} \quad \text{and} \quad \boldsymbol{q}_i = \mathcal{R} \boldsymbol{p}_i + \boldsymbol{t}, \tag{4}$$

where q_i, r_i and h_i denote respectively the integer pin position on the bottom plate grid and its height, and δ is the jaw separation.

Equation (4) is a condition for contact between pin number i and the corresponding face. It can be rewritten as $\mathcal{C}_i(x, y, \theta, \delta) = 0$, where

$$\mathcal{C}_i(x, y, \theta, \delta) \overset{\text{def}}{=} (x - q_i)\cos(\theta + \alpha_i) + (y - r_i)\sin(\theta + \alpha_i) + d_i \delta - e_i = 0, \tag{5}$$

and $\alpha_i = \mathrm{Arg}(a_i, b_i)$ and $d_i = 1/\sqrt{a_i^2 + b_i^2}$, and $e_i = d_i(c_i + h_i)$.[1] Note that α_i is simply the angle between the u axis and the projection of $\boldsymbol{n}_i$ onto the u, v plane (Figure 3).
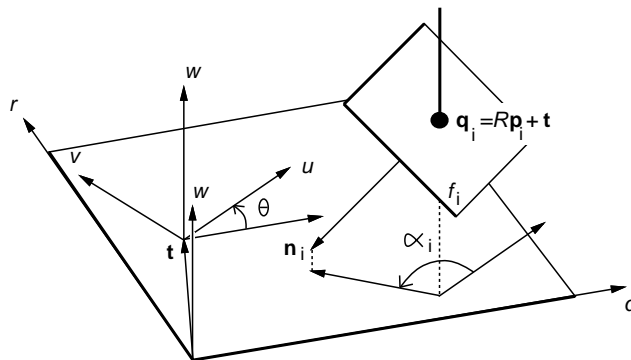
Figure 3: Contact between a pin and a face.

---

[1] Here, abusing the usual mathematical notation, $\mathrm{Arg}(c, s)$ is the angle a such that $\cos(a) = c/\sqrt{c^2 + s^2}$ and $\sin(a) = s/\sqrt{c^2 + s^2}$.

The three pins will be in contact with the corresponding faces when (5) is satisfied for $i = 1, 2, 3$. In particular, any linear combination $\sum_{i=1}^{3} \xi_i \mathcal{C}_i(x, y, \theta, \delta)$ of the contact constraints will also be equal to zero. In particular, if we choose $\xi_i = \mu_i/(d_i l_i)$, we can use the relation $\boldsymbol{n} = -\sum_{i=1}^{3} \mu_i \boldsymbol{n}_i$ to eliminate the variables x and y. We obtain

$$\mathcal{E}(\delta, \theta) \stackrel{\text{def}}{=} \sum_{i=1}^{3} \frac{\mu_i}{d_i l_i} \mathcal{C}_i(x, y, \theta, \delta) = \delta - A\cos(\theta - \alpha) - B, \tag{6}$$

where

$$\begin{cases} A = \sqrt{C^2 + S^2}, \quad \alpha = \text{Arg}(C, S), \quad B = \sum_{i=1}^{3} \frac{\mu_i}{l_i}(c_i + h_i), \\[2mm] C = \sum_{i=1}^{3} \frac{\mu_i}{l_i}(a_i q_i + b_i r_i), \quad \text{and} \quad S = \sum_{i=1}^{3} \frac{\mu_i}{l_i}(-b_i q_i + a_i r_i). \end{cases}$$

Note that the notation $\mathcal{E}(\theta, \delta)$ is justified by the fact that the value of $\mathcal{E}$ is independent of x and y. More importantly, it is now clear that a necessary condition for the existence of an object position achieving contact with the three pins is that the point (θ, δ) lies on the *contact sinusoid* defined by $\mathcal{E}(\delta, \theta) = 0$. This condition is also sufficient: for given values of θ and δ on this sinusoid, the three linear equations $\mathcal{C}_i(x, y, \theta, \delta)$ $(i = 1, 2, 3)$ in the two unknowns x and y are linearly dependent, and thus admit a common solution.

2.1.2 Equilibrium

The equilibrium equation (1) expresses both force and moment equilibrium. Using (4) and exploiting the fact that the overall scale of the wrenches is irrelevant allows us to rewrite the moment equilibrium equation as

$$\sum_{i=1}^{3} \lambda_i(\boldsymbol{v}_i \times \boldsymbol{n}) + \sum_{i=1}^{3} \mu_i[(\mathcal{R}^{-1}(\boldsymbol{q}_i - \boldsymbol{t})) \times \boldsymbol{n}_i] = 0, \quad \text{with} \quad \lambda_1 + \lambda_2 + \lambda_3 = 1 \quad \text{and} \quad \lambda_1, \lambda_2, \lambda_3 \geq 0. \tag{7}$$

In this case, the force equilibrium equation is simply the relation $\boldsymbol{n} = -\sum_{i=1}^{3} \mu_i \boldsymbol{n}_i$ established earlier. Using this relation and writing the dot product of the contact moments and $\boldsymbol{n}$ in the (u, v, w) coordinate system yields

$$\sum_{i=1}^{3} \frac{\mu_i}{l_i}[(-b_i q_i + a_i r_i)\cos\theta - (a_i q_i + b_i r_i)\sin\theta] = 0 \iff \sin(\theta - \alpha) = 0.$$

It follows that a necessary condition for three pins in contact with the corresponding faces of the object to achieve equilibrium is that $\theta = \alpha$ or $\theta = \alpha + \pi$. Note that these values of θ are independent of the heights of the pins, which will prove extremely important in the grasp planning algorithm presented in Section 2.2.

The above condition is only necessary. However, for a given object/gripper configuration (i.e., assuming that the pin positions and heights, the jaw separation, and the object position and orientation are known), we can compute the coefficients λ_i from the equation $\lambda_1 + \lambda_2 + \lambda_3 = 1$ and the two components of the moment equilibrium equation along the u, v axes. If these coefficients are positive, then the grasp will achieve equilibrium.

Note that we could have used the same line of reasoning if f had been an arbitrary convex polyhedron with $k > 3$ edges. In this case however, the coefficients λ_i $(i = 1, .., k)$ are not uniquely determined by (7), which contradicts the notion of essential equilibrium required by Rimon's and

7

Burdick's second-order mobility theory. This is our reason for assuming that f is triangular in this section. Note however, that (non-essential) equilibrium can still be tested in this case using linear programming to determine whether the constraints (7) admit a solution. In addition, the refined geometric analysis of Section 3 will show that essential equilibrium is not necessary for immobility in the case of our gripper, which will allow us to abandon the triangular face assumption.

2.1.3   Immobility

We now examine the sufficient condition for immobility (2) in the case of our gripper. Since the radii corresponding to the planar contacts are effectively infinite, it is obvious that $\boldsymbol{\omega}^T \mathcal{K} \boldsymbol{\omega}$ is negative for any vector $\boldsymbol{\omega}$ which is not parallel to $\boldsymbol{n}$. Thus we must determine the sign of

$$\boldsymbol{n}^T \mathcal{K} \boldsymbol{n} = M \sum_{i=1}^{3} \mu_i [(\boldsymbol{n}_i \times \boldsymbol{n}) \cdot (\boldsymbol{P}_i \times \boldsymbol{n}) - r|\boldsymbol{n}_i \times \boldsymbol{n}|^2], \tag{8}$$

where r is the common radius of the pins and $M = 1/(1 + \sum_{i=1}^{3} \mu_i)$ is a scale factor used to balance the fact that we have chosen $\lambda_1 + \lambda_2 + \lambda_3 = 1$ in our formulation of equilibrium. Note that we have used $\boldsymbol{P}_i$ instead of $\boldsymbol{p}_i$ to denote the position of the contact point because (2) and (8) are valid in the coordinate system of the *original object*: as noted earlier, we assume in the rest of this paper that the object has been grown by the pin radius, while the spherical end of the pin has been shrunk into its center. This implies that $\boldsymbol{P}_i = \boldsymbol{p}_i + r\boldsymbol{n}_i$. In turn, using (4) allows us to rewrite (8) as

$$\boldsymbol{n}^T \mathcal{K} \boldsymbol{n} = M \sum_{i=1}^{3} \mu_i (\boldsymbol{n}_i \times \boldsymbol{n}) \cdot [(\mathcal{R}^{-1}(\boldsymbol{q}_i - \boldsymbol{t})) \times \boldsymbol{n}],$$

or equivalently

$$\boldsymbol{n}^T \mathcal{K} \boldsymbol{n} = M \sum_{i=1}^{3} \frac{\mu_i}{l_i} [(a_i q_i + b_i r_i) \cos \theta + (-b_i q_i + a_i r_i) \sin \theta] = AM \cos(\theta - \alpha),$$

and it follows that $\mathcal{K}$ is negative definite if and only if $\theta = \alpha + \pi$.

2.1.4   Main Results

We can now summarize the results obtained in this section with the following lemma.

Lemma 1: For given integer pin positions and heights q_i, r_i and h_i ($i = 1, 2, 3$), a sufficient condition for an object at configuration (x_0, y_0, θ_0) to be immobilized by a grasp with jaw separation δ_0 is that:

(1) $\theta_0 = \alpha + \pi$,

(2) $\mathcal{C}_i(x_0, y_0, \theta_0, \delta_0) = 0$ for $i = 1, 2, 3$,

(3) if $\mathcal{R}_0$ denotes the rotation of angle θ_0 about $\boldsymbol{n}$, and $\boldsymbol{t}_0$ denotes the translation (x_0, y_0), the points $\mathcal{R}_0(\boldsymbol{q}_i - \boldsymbol{t}_0)$ satisfy the inequalities (3) for $i = 1, 2, 3$, and

(4) the constraints (7) on the coefficients λ_i ($i = 1, 2, 3$) admit a positive solution.

This lemma is an obvious corollary of the results obtained in Sections 2.1.1, 2.1.2 and 2.1.3, the third condition simply expressing the fact that the contacts must occur within the faces.

2.2   Algorithm

According to Lemma 1, all continuous degrees of freedom of a grasp (object orientation, jaw sep-
aration and object position) can be computed once the grasp's discrete degrees of freedom (pin
positions and heights) have been set. This yields the following naive algorithm for grasp planning:
for each quadruple of faces, enumerate all grid positions and heights of the three pins, then compute
the remaining grasp parameters and check whether they satisfy conditions (3) and (4) of Lemma
1. The complexity of this algorithm is obviously $O(N^4 D^6)$, where N is the number of faces of
the grasped polyhedron, and D is its diameter measured in units equal to the distance between
successive grid points.

A better approach is the following algorithm, which has the same overall structure as the naive
one, but limits the number of faces and gripper configurations under consideration by exploiting a
number of geometric constraints, most notably the fact that the orientation of an object held in an
immobilizing grasp depends only on the pins' positions and not on their heights:

For each quadruple of faces do

(1) Test whether they can be held in equilibrium.

(2) Enumerate all pin positions that may hold the object in equilibrium and compute the corre-
sponding object orientation.

(3) For each such position, enumerate the pin lengths that immobilize the object and compute
the remaining grasp parameters.

(4) Compute the corresponding coefficients λ_i and check that they are positive.

The first step of the algorithm uses linear programming and polytope projection techniques
[14, 22, 21, 38] to prune gripper configurations that cannot achieve equilibrium. The second step
uses distance constraints to reduce the enumeration of the pin positions that may yield equilibrium
grasps to the scan-line conversion of circular shells (see [4, 5, 51, 52] for related approaches to
fixture planning for two-dimensional objects). The third step of the algorithm uses condition (3) of
Lemma 1 to reduce the enumeration of pin heights that yield immobilizing grasps to polygon scan
conversion. Finally, the fourth step uses (7) to compute the coefficients λ_i and make sure they are
positive.

Steps 1 to 3 of the algorithm are detailed in Sections 2.2.1 to 2.2.3. Section 2.2.4 shows that its
complexity is $O(N^4 D^2 d^4)$ where d is the maximum diameter of the object's faces (note that $d \leq D$,
and that for polyhedra with many faces having roughly the same area, d is in general much smaller
than D). Empirical results are presented in Section 2.3.

2.2.1   Testing the Existence of Equilibrium Configurations

We first check that the four surface normals positively span $\mathbb{R}^3$. This is easily done by checking
that any three of the normals are linearly independent, then using the equation $\boldsymbol{n} = -\sum_{i=1}^{3} \mu_i \boldsymbol{n}_i$ to
compute the coefficients μ_i and test whether they have the same sign. If they do not, the quadruple
of faces under consideration is rejected. If they do, the normals positively span $\mathbb{R}^3$, and (7) provides
four linear equations in the the nine unknowns λ_i, u_i, v_i $(i = 1, 2, 3)$.

We can now test the existence of equilibrium configurations by using linear programming to
determine whether the five-dimensional polytope defined by (7) and the inequality constraints (3)
and $\lambda_i \geq 0$ is empty. When this polytope is not empty, there is only (in general) a subset of each

face that can participate in an equilibrium configuration. The subset corresponding to face number i is determined by projecting the polytope defined onto the plane (u_i, v_i).

Several algorithms can be used to perform this projection, including Fourier's method [14], the convex hull and extreme point approaches of Lassez and Lassez [22, 21], and the Gaussian elimination and contour tracking techniques of Ponce *et al.* [38]. For faces with a bounded number of edges, all of these algorithms run in constant time, and they can be used to construct subsets of the original faces that are then passed as input to the rest of the algorithm. As noted earlier, this projection process affords an early pruning of gripper configurations that cannot achieve equilibrium and therefore immobilization.

2.2.2 Enumerating Pin Positions

As shown by Lemma 1, given a quadruple of faces, we can first enumerate all possible pin locations on the lower plate and compute the corresponding rotations, then enumerate the corresponding pin heights and compute the corresponding jaw separation and object pose.

An exhaustive search of all possible grid coordinates would be extremely expensive: consider an object of diameter D (measured in units equal to the distance between successive grid points); there are a priori $O(D^4)$ different pin locations, since we can position one pin at the origin and the other two pins at arbitrary locations on the grid. Instead, we use an approach similar to the algorithms presented by Wallack and Canny [51, 52] and Brost and Goldberg [4], using bounds on the distance between two faces to restrict the set of grid coordinates under consideration. Clearly, each pin must lie within the horizontal projection of each face. Thus if we position the first pin at the origin, the integer point corresponding to the second pin is constrained to lie within the circular shell centered at the origin with inner radius equal to the minimum distance between the projections of the two corresponding faces and outer radius equal to the maximum distance. Given the position of the second pin, the third pin is now constrained to lie within the region formed by the intersection of the two shells associated with the first and second pin.

Enumerating the pin locations thus amounts to determining the integer positions falling in planar regions defined by a circular shell or the intersection of two such shells. This can be done in optimal time proportional to the number of these points by using a scan-line conversion algorithm (Figure 4).
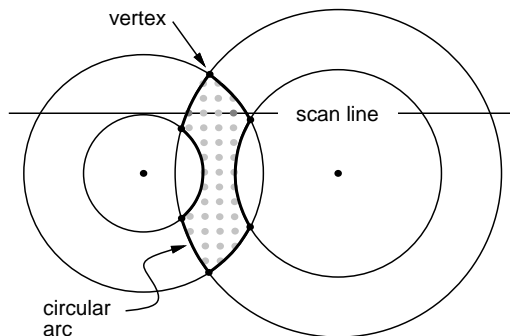
Figure 4: Scan-line conversion: spans between consecutive boundary elements are filled one scan-line at a time.

2.2.3 Enumerating Pin Heights

Once the position of the pins has been chosen and the corresponding rotation has been computed, we can align the gripper's and object's coordinate systems so they are only separated by the horizontal translation (x, y). This allows us to rewrite the contact equations as

$$a_i(x - q_i) + b_i(y - r_i) + \delta - c_i - h_i = 0 \quad \text{for} \quad i = 1, 2, 3. \tag{9}$$

Equation (9) holds whenever the three pins are in the planes of the faces f_i of the grasped object. Writing that the pins actually lie within the faces constrains the possible values of the translation $\boldsymbol{t}$ between the gripper and object coordinate frames: let us denote by by f_i' the convex polygon $\{(x, y) | a_{ij}(x - q_i) + b_{ij}(y - r_i) - c_{ij} \geq 0 \text{ for } j = 1, .., k_i\}$ (geometrically, f_i' can be constructed by projecting f_i onto the (u_i, v_i) plane, then applying to the projection a symmetry with respect to the origin and a translation by (q_i, r_i)). Using once again (4) shows that the point (x, y) is restricted to lie within the polygon $F' = f_1' \cap f_2' \cap f_3'$ (Figure 5(a)). Substituting into (9) and using the fact that we can choose $q_1 = r_1 = h_1 = 0$ now yields

$$\begin{pmatrix} h_2 \\ h_3 \end{pmatrix} \in \{\mathcal{A} \begin{pmatrix} x \\ y \end{pmatrix} + \boldsymbol{b} | \begin{pmatrix} x \\ y \end{pmatrix} \in F'\},$$

where

$$\mathcal{A} = \begin{pmatrix} a_2 - a_1 & b_2 - b_1 \\ a_3 - a_1 & b_3 - b_1 \end{pmatrix}, \ \boldsymbol{b} = \begin{pmatrix} c_1 - (a_2 q_2 + b_2 r_2 + c_2) \\ c_1 - (a_3 q_3 + b_3 r_3 + c_3) \end{pmatrix}.$$
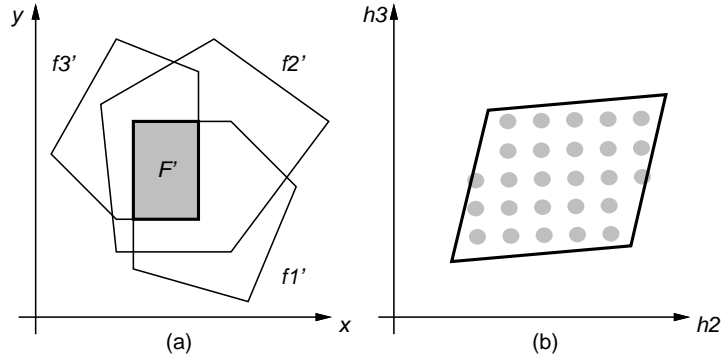
Figure 5: Enumerating pin lengths: (a) the polygon F' defined in the x, y plane by the intersection of the faces f_i', and (b) the corresponding convex polygon in the h_2, h_3 plane, along with the integer points inside it.

In other words, the possible values of (h_2, h_3) are simply the integer points that lie in the polygon defined by the above equation, which is obtained from F' by an affine transformation (Figure 5(b)). These points can once again be determined in optimal time proportional to their actual number using a polygon scan-line conversion algorithm.

Now, for a given configuration (location plus length) of the pins, (9) forms a system of three linear equations in the three variables x, y, and δ. This system is readily solved to yield the pose of the object and the separation of the plates. Note as before that the values of the coefficients λ_i are easily computed from (7) at this point.

Note that the gripper configurations found by our algorithm will automatically ensure that the contacts between the three pins and the planes of the corresponding faces occur within the faces.

2.2.4　Algorithm Analysis

As noted earlier, the complexity of the naive algorithm is $O(N^4 D^6)$. Let us assume without loss of generality that each face can be inscribed in a disc of diameter d (note that $d \leq D$ and that in practice, we will often have $d \ll D$). The area of a circular shell is then $O(Dd)$, and the area of the intersection of two such shells is also at worse $O(Dd)$. Finally, the area of the polygon F' is $O(d^2)$. Thus the total complexity of the algorithm is $O(N^4 D^2 d^4)$. As noted in Section 1, this is an improvement over the algorithm proposed in [35, 49], whose complexity is $O(N^4 D^4 d^2)$ since it does not decouple the enumeration of the pin positions and pin heights.

To obtain a more realistic estimate of our algorithm's behavior, let us consider a polyhedron with total area A whose faces all have the same area, so $d^2 = O(D^2/N) = O(A/N)$. Under this assumption, the complexity of our algorithm is $O(N^2 A^3)$. It should also be noted that in practice, when $d \ll D$, the area of the intersection of two circular shells will often be proportional to d^2 rather than Dd. Of course, this does not change the worst-case complexity of the algorithm.

2.3　Implementation and Results

The implementation has been written in C. Figures 6 and 7 show some of the grasps of a tetrahedron and of a polyhedron with 10 faces that our algorithm has found using a 5×5 grid.

(a)　　　　　　　　　　　　　　　(b)

(c)
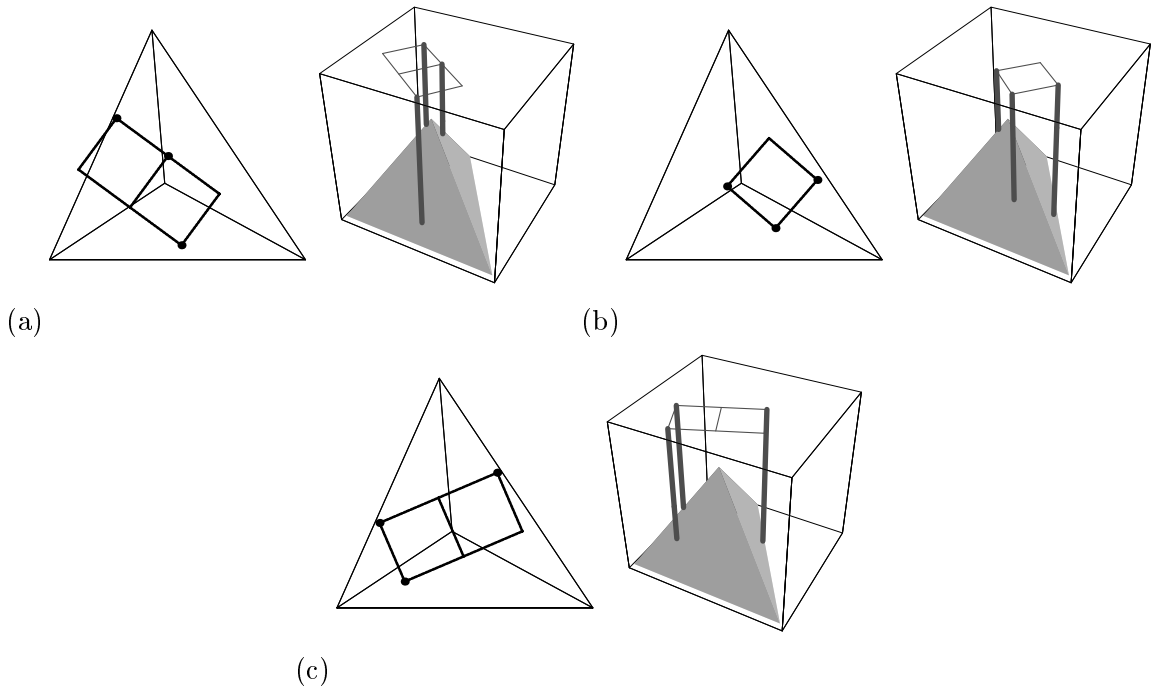
Figure 6: Grasping a tetrahedron: some solutions for a 5×5 grid.

Table 1 gives some quantitative results. We have used a $K \times K$ grid with various values of K, as well as pins whose height may take ten discrete values. The table shows the results obtained without any pruning (N), using circular shell pruning only (S), and combining the projection- and shell-pruning stages (P+S). The last column (G) shows the number of these configurations that actually yield immobilizing grasps. All run times have been measured on a SUN SPARCstation 10. The table shows that, as could be expected, pruning eliminates a much larger percentage of the possible configurations in the case of the polyhedron with 10 faces than in the case of
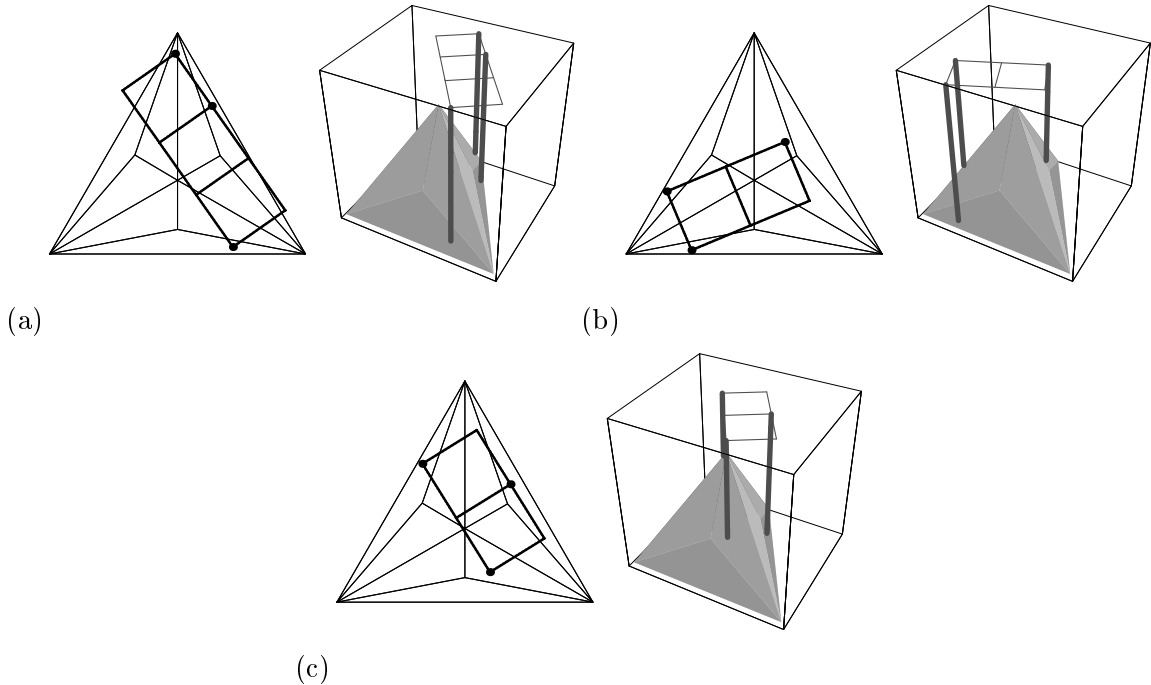
Figure 7: Grasping a 10-face polyhedron: some solutions for a 5×5 grid.

the tetrahedron, corresponding to the fact that, for most choices of faces, the range between the minimum and maximum distances is smaller for the polyhedron with 10 faces.

3 In-Hand Manipulation

We present a new approach to in-hand manipulation based on the concept of *inescapable configuration space* (ICS) region , i.e., on the idea of characterizing the regions of configuration space for which the object is not immobilized but is constrained to lie within a bounded region of the free configuration space (see [42] for related work in the two-dimensional, two-finger case). As noted in Section 1, this allows us to generalize the notion of grasp stability to finite-size displacements.

ICS regions will also allow us to plan in-hand object motions as sequences of gripper configurations (see [1, 12, 16, 24, 26, 40, 42] for related work): starting from some immobilizing configuration, we can open the gripper jaws and retract the immobilizing pins, then choose another triple of pins whose ICS region contains the initial gripper configuration, lower these pins, and as the jaws close, move the object to the corresponding immobilized configuration. Note that this approach does not require modeling what happens when contact occurs, but it indeed requires frictionless contacts to avoid wedging. We will assume in the rest of this section that the quadruple of faces under consideration is fixed.

3.1 Geometry of the Problem

3.1.1 Free Configuration Space Regions

Let us consider an immobilizing configuration of the gripper, defined by the position q_i, r_i and height h_i of the pins ($i = 1, 2, 3$), by the position x_0, y_0 and orientation θ_0 of the object in the

Tetrahedron							
K	Number of	Run Time (s)			Number of Candidates			
	Solutions	N	S	P+S	N	S	P+S	G
3	0	1	1	1	33	10	10	0
4	160	1	1	1	141	42	40	10
5	704	2	1	2	411	145	135	52
6	1,963	4	2	2	927	391	378	131
7	4,263	8	4	4	1,839	795	751	255
Polyhedron with 10 Faces								
K	Number of	Run Time (s)			Number of Candidates			
	Solutions	N	S	P+S	N	S	P+S	G
3	0	20	1	2	2,772	750	712	0
4	189	47	3	4	11,844	2,213	2,102	42
5	794	72	9	9	34,524	3,819	3,537	171
6	2,326	142	20	20	77,868	7,811	7,125	544
7	5,046	341	43	41	154,476	16,259	14,951	1,519

Table 1: Quantitative results for two test objects.

gripper's coordinate system, and by the jaw separation δ_0. We assume that the values of q_i, r_i and h_i are held constant and examine what happens when the separation of the jaws changes.

For a given jaw separation δ, the set $S_i(\delta)$ of object configurations (x, y, θ) for which $C_i(x, y, \theta, \delta) = 0$ forms a ruled surface: indeed, its intersection with a plane $\theta = \text{constant}$ is a line $L_i(\delta, \theta)$ at distance $e_i - d_i\delta$ from the fixed point (q_i, r_i) of the x, y plane, and the angle between the x axis and the normal to this line is $\theta + \alpha_i$ (Figure 8). Changing θ corresponds to rotating the line about the point (q_i, r_i), while changing δ corresponds to translating the line.
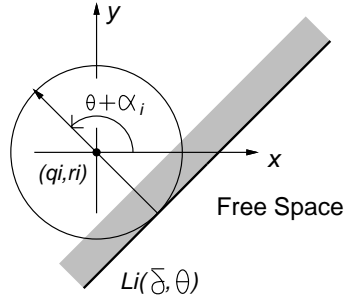
Figure 8: Contact between a pin and a face in configuration space.

The ruled surface $S_i(\delta)$ splits the three-dimensional space $\mathbb{R}^2 \times S^1$ of configurations x, y, θ into a "free" half-space $V_i(\delta)$ and a "forbidden" half-space $W_i(\delta)$ where pin number i penetrates the plane of f_i. Furthermore, $V_i(\delta)$ (resp. $W_i(\delta)$) is characterized by $C_i(x, y, \theta, \delta) \geq 0$ (resp. ≤ 0).

Now let us consider the volume $V(\delta) = V_1(\delta) \cap V_2(\delta) \cap V_3(\delta)$. Given the form of $C_i(x, y, \theta, \delta)$, it is obvious that if a configuration lies in free space for some value δ_1 of δ, it also lies in free space for any other value $\delta_2 \geq \delta_1$. In other words, $V(\delta_1) \subset V(\delta_2)$ when $\delta_2 \geq \delta_1$ (this is also intuitively obvious since increasing δ corresponds to opening the jaws). In particular, the immobilizing configuration (x_0, y_0, θ_0) is always in free space for $\delta \geq \delta_0$.

The intersection of $V(\delta)$ with a plane $\theta = \text{constant}$ forms a triangular region $T(\delta, \theta)$. Note that the triangles corresponding to various values of θ are all homothetic since their edges make

constant angles with each other. However, their size, position, and orientation varies with θ. Note also that these triangles, although possibly empty, are not degenerate: indeed, it is easy to verify that a necessary and sufficient for two edges of $T(\delta, \theta)$ to be parallel is that the normals to the corresponding faces be either equal or symmetric with respect to the vector $\boldsymbol{n}$, which contradicts the assumption that the directions $\boldsymbol{n}_i$ ($i = 1, 2, 3$) and $\boldsymbol{n}$ positively span $\mathbb{R}^3$.

As shown in Figure 9, the region $T(\delta, \theta)$ may contain an open subset (Figure 9(a)), be reduced to a single point (Figure 9(b)), or be empty (Figure 9(c)).
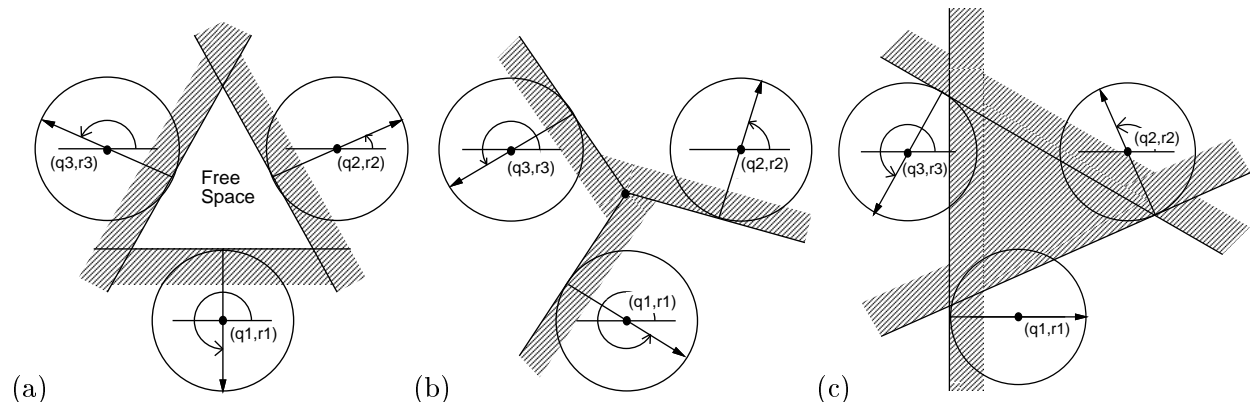
Figure 9: Possible configurations of the intersection $T(\delta, \theta)$ of $V(\delta)$ with a plane $\theta = $ constant: (a) $T(\delta, \theta)$ contains an open neighborhood; (b) it is reduced to an isolated point of the x, y plane; (c) it is empty.

In the second case (Figure 9(b)), the three pins simultaneously touch the corresponding faces, and $\mathcal{E}(\delta, \theta) = 0$. In fact, it is easy to show that a necessary and sufficient condition for $T(\delta, \theta)$ to contain at least one point is that $\mathcal{E}(\delta, \theta) \geq 0$: the condition is clearly necessary: since $\mathcal{E}(\delta, \theta)$ is by construction a convex combination of the functions $\mathcal{C}_i(x, y, \theta, \delta)$, the fact that $\mathcal{E}(\delta, \theta) < 0$ implies that, for any x, y, there exists some $i \in \{1, 2, 3\}$ such that $\mathcal{C}_i(x, y, \theta, \delta) < 0$. To show that the condition is also sufficient, let us assume that $T(\delta, \theta)$ is empty. This implies that, for any x, y, there exists some $i \in \{1, 2, 3\}$ such that $\mathcal{C}_i(x, y, \theta, \delta) < 0$. In particular, if (x_{12}, y_{12}) is the point where the two lines associated with the faces f_1 and f_2 intersect (as remarked earlier, these lines are not parallel), we must have $\mathcal{E}(\delta, \theta) = (\mu_3/d_3 l_3) C_3(x_{12}, y_{12}, \theta, \delta) < 0$.

This result allows us to characterize qualitatively the range of orientations θ for which $T(\delta, \theta)$ is not empty (Figure 10): for a given δ, the condition $\mathcal{E}(\delta, \theta) = 0$ is an equation in θ that may have zero, one, or two real solutions: a double root occurs at the minimum $\delta = \delta_0$ or at the maximum $\delta = \delta_{\max}$ of the sinusoid. In the former case, $\mathcal{E}$ is strictly positive everywhere except at $\theta = \alpha$ where it is equal to zero, and the range of orientations is S^1. In the latter case, the range of orientations reduces to a single point $\theta_0 = \alpha + \pi$. For any value δ_1 in the open interval $]\delta_0, \delta_{\max}[$, there are two distinct roots θ', θ'', and the range of orientations is the arc bounded by these roots and containing θ_0. Finally, for values of δ outside the $[\delta_0, \delta_{\max}]$ interval, there is no solution: either δ is strictly smaller than δ_0 and the range of orientations is empty (at least one of the pins penetrates the plane of the corresponding face), or δ is strictly larger than $\delta_{\max}$, and the range of orientations is S^1.

In particular, since the volume $V(\delta)$ is a stack of contiguous triangles $T(\delta, \theta)$, it is clear at this point that, for $\delta \geq \delta_0$, $V(\delta)$ is a non-empty, connected, compact region of $\mathbb{R}^2 \times S^1$. The analysis conducted in this section also gives some geometric insight on the immobility conditions derived earlier. In particular, it confirms that the minimum point $(\alpha + \pi, \delta_0)$ of the contact sinusoid corresponds to an isolated point of configuration space or equivalently to an immobilizing configuration:
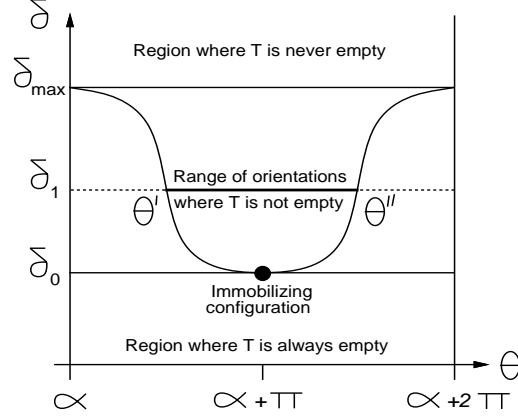
Figure 10: Regions of θ, δ space delimited by the sinusoid $\mathcal{E}(\delta, \theta) = 0$.

indeed, the triangle $T(\delta_0, \alpha + \pi)$ is reduced to a point, and $T(\delta, \theta)$ is empty for any $\theta \neq \theta_0$. Likewise, although the maximum $(\alpha, \delta_{\max})$ of the sinusoid corresponds to an equilibrium grasp, it does not yield an immobilizing grasp since the object is free to undergo arbitrary rotations.

Note also that the above analysis does not rely in any way on the contact wrenches being in *essential* equilibrium. Thus we have kept our promise, and shown that the grasp planning approach presented in Section 2 can be extended to handle arbitrary convex polygons. This only requires two simple modifications of the grasp planning algorithm: first, step (1) of the algorithm now requires computing the projection of a $k + 2$-dimensional polytope onto a plane, where k is the number of edges bounding the bottom face f. Second, since the coefficients λ_i $(i = 1, .., k)$ are not uniquely determined by (7) for faces with $k > 3$ edges, step (4) of the algorithm now requires using linear programming to check that there exists a set of nonnegative coefficients λ_i satisfying (7). For faces with a bounded number of edges, these two modifications do not change the overall complexity of the algorithm.

3.1.2 Inescapable Configuration Space Regions

The discussion so far has characterized the contacts between the pins and the planes of the corresponding faces, ignoring the fact that each face is in fact a convex polygon in its plane. Let us construct a parameterization of the set $E_i(\delta, \theta)$ of configurations (x, y) for which the tip of pin number i belongs to the corresponding face. Obviously, $E_i(\delta, \theta)$ is a subset of $L_i(\delta, \theta)$. This line is at distance $-d_i\delta + e_i$ from the point (q_i, r_i), with a normal whose orientation is $\theta + \alpha_i$; hence, it can be parameterized by

$$\begin{pmatrix} x \\ y \end{pmatrix} = \begin{pmatrix} q_i \\ r_i \end{pmatrix} + (-d_i\delta + e_i) \begin{pmatrix} \cos(\theta + \alpha_i) \\ \sin(\theta + \alpha_i) \end{pmatrix} + \eta \begin{pmatrix} -\sin(\theta + \alpha_i) \\ \cos(\theta + \alpha_i) \end{pmatrix}, \quad \eta \in \mathbb{R}.$$

Using this parameterization and (4) yields

$$\begin{pmatrix} u_i \\ v_i \end{pmatrix} = (d_i\delta - e_i) \begin{pmatrix} \cos\alpha_i \\ \sin\alpha_i \end{pmatrix} - \eta \begin{pmatrix} -\sin\alpha_i \\ \cos\alpha_i \end{pmatrix}.$$

In turn, substituting these values in the inequalities (3) defining f_i yields a set of linear inequalities in η and δ. Actual contact occurs for pairs (η, δ) lying in the convex polygon defined by these constraints. It follows that for given values of δ and θ, $E_i(\delta, \theta)$ is a line segment, and the parameters η' and η'' associated with its endpoints are piecewise-linear functions of δ.

16

Now let us consider the three segments $E_i(\delta, \theta)$ ($i = 1, 2, 3$) together (Figure 11): if $E_i(\delta, \theta)$ and $E_j(\delta, \theta)$ intersect for all $i \neq j$, then the three segments completely enclose the triangle $T(\delta, \theta)$ (Figure 11(a)). We say that the corresponding configuration satisfies the *enclosure condition* since there is no escape path for the object in the x, y plane with the corresponding orientation θ. More generally, when all triples of segments in the range of orientations associated with a given jaw separation δ satisfy the enclosure condition, $V(\delta)$ itself is an *inescapable configuration space* (ICS) region: in other words, the object is free to move within the region $V(\delta)$, but remains imprisoned by the grasp and cannot escape to infinity.
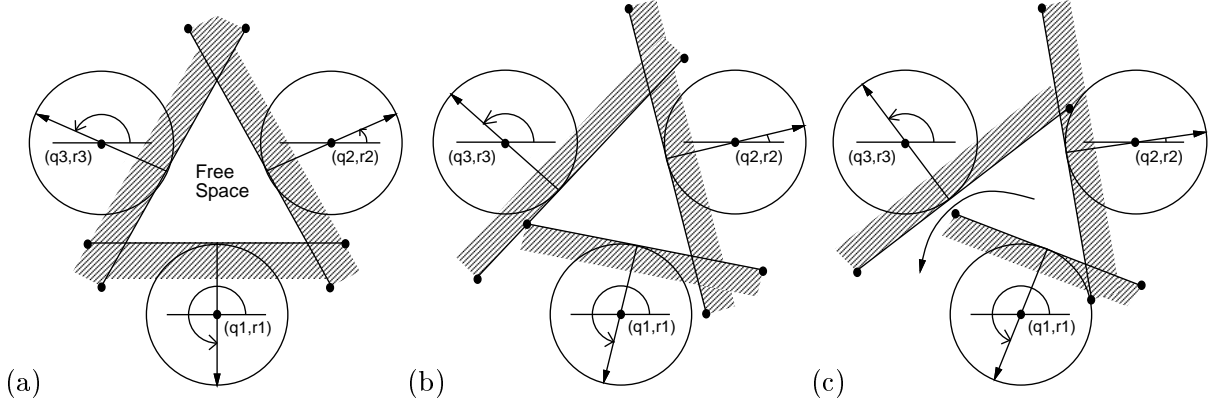
Figure 11: Triangle configurations: (a) three segments enclosing a triangle; (b) a critical configuration; (c) an opened triangle and an escape path.

3.1.3 Maximum ICS Regions

Here we address the problem of characterizing the maximum value δ^* for which $V(\delta)$ forms an ICS region for any δ in the $[\delta_0, \delta^*]$ interval. We know that at $\delta = \delta_0$ the three segments intersect at the immobilizing configuration, forming an ICS region reduced to a single point. Thus the enclosure condition holds at $\delta = \delta_0$. On the other hand, as $\delta \to +\infty$, the whole configuration space becomes free of obstacles, thus there must exist a critical point for some minimal value of δ greater than δ_0. This guarantees that δ^* has a finite value.

As shown by Figure 11(b), a critical event occurs when one of the endpoints of a segment lies on the line supporting another segment. After this event, the line segments fail to enclose the triangle $T(\delta, \theta)$ and the object can escape the grasp (Figure 11(c)).

According to the results established in the previous section, we can parameterize the coordinates of one of the endpoints of the segment $E_i(\delta, \theta)$ by

$$\begin{pmatrix} x \\ y \end{pmatrix} = \begin{pmatrix} q_i \\ r_i \end{pmatrix} + (-d_i\delta + e_i) \begin{pmatrix} \cos(\theta + \alpha_i) \\ \sin(\theta + \alpha_i) \end{pmatrix} + (f_i\delta + g_i) \begin{pmatrix} -\sin(\theta + \alpha_i) \\ \cos(\theta + \alpha_i) \end{pmatrix}, \qquad (10)$$

on the appropriate δ interval, with constants f_i and g_i determined by the coefficients a_{ij}, b_{ij} and c_{ij} of (3).

A critical event occurs when the endpoint under consideration is on the line $L_j(\delta, \theta)$ for some $j \neq i$. Substituting (10) into (5) yields, after some simple algebraic manipulation

$$A_{ij} \cos(\theta + \beta_{ij}) + B_{ij}\delta + C_{ij} = 0, \qquad (11)$$

where

$$\begin{cases} A_{ij} = \sqrt{(q_i - q_j)^2 + (r_i - r_j)^2}, \\ \beta_{ij} = \alpha_j - \mathrm{Arg}(q_i - q_j, r_i - r_j), \\ B_{ij} = d_j - d_i \cos(\alpha_j - \alpha_i) + f_i \sin(\alpha_j - \alpha_i), \\ C_{ij} = -e_j + e_i \cos(\alpha_j - \alpha_i) + g_i \sin(\alpha_j - \alpha_i). \end{cases}$$

In other words, critical configurations form a second sinusoid in θ, δ space, called the *critical sinusoid* in the rest of this presentation.

We seek the minimum value of $\delta^* > \delta_0$ for which the range of orientations includes one of the critical orientations. As discussed above, we know that δ^* exists. Let us suppose first that a critical value lies in the interior of the range of orientations associated with some $\delta_1 \geq \delta_0$, and denote by $\delta_{\min}$ the minimum value of δ on the critical sinusoid. By definition, we have $\delta_1 \geq \delta_{\min}$. Suppose that $\delta_1 > \delta_{\min}$. Then by continuity, there exists some δ_2 such that $\delta_{\min} < \delta_2 < \delta_1$ and the corresponding range of orientations also contains a critical orientation (Figure 12). The argument holds for any value of $\delta > \delta_{\min}$. In other words, either the range of orientations of $\delta_{\min}$ contains a critical orientation, in which case $\delta^* = \delta_{\min}$ (Figure 12(a)), or it does not, in which case the critical value associated with δ^* must be one of its range's endpoints (Figure 12(b)). This is checked by intersecting the contact sinusoid and the critical one. Note that this process must be repeated six times (once per each segment/vertex pair) to select the minimum value of δ^*.
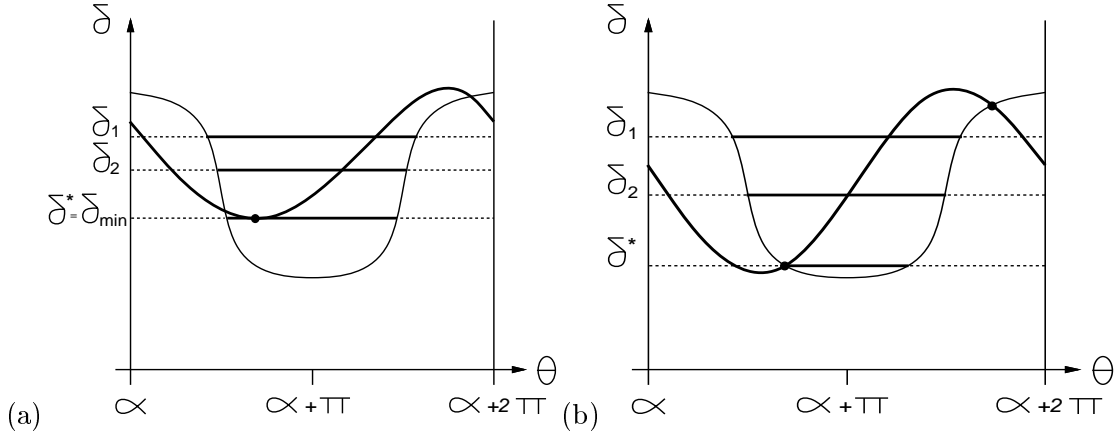
Figure 12: Critical configurations: (a) the critical configuration is the minimum of the critical sinusoid (shown as the thicker curve); (b) the critical configuration is the minimum intersection of the critical sinusoid and the contact sinusoid.

3.1.4   Main Result

The following lemma follows immediately from the results established in Sections 3.1.1, 3.1.2 and 3.1.3 and summarizes the findings of these sections.

Lemma 2: For given integer pin positions and heights q_i, r_i and h_i ($i = 1, 2, 3$) and an immobilizing configuration $(x_0, y_0, \theta_0, \delta_0)$, there exists a critical jaw separation δ^* such that:

(1) for any $\delta > \delta^*$, there exists a path allowing the object to escape the grasp,

(2) for any δ in the interval $[\delta_0, \delta^*]$, the volume $V(\delta)$ is an inescapable region of configuration space that contains the configuration $(x_0, y_0, \theta_0, \delta_0)$,

18

(3) for any $\delta' \leq \delta''$ in the interval $[\delta_0, \delta^*]$, $V(\delta') \subset V(\delta'')$, and

(4) δ^* can be computed in closed form as the minimum of a sinusoid or the intersection of two sinusoids.

3.2   Algorithm

Lemma 2 can be used as a basis for in-hand manipulation by remarking that an object anywhere in the ICS region associated with some gripper configuration can be moved to the corresponding immobilized position and orientation by closing the gripper jaws (this follows immediately from properties (2) and (3) in Lemma 2). Thus we can plan manipulation sequences from one immobilized configuration to another by using the following algorithm:

Off-line:

(1) Compute the set S of all immobilizing configurations of the object.

(2) Construct a directed graph G whose vertices are the elements of S and whose edges are the pairs (s, s') of elements of S such that s belongs to the maximum ICS region ICS(s') associated with s'.

On-line:

(3) Given two configurations i and g in S, search the graph G for the shortest path going from the initial configuration i to the goal configuration g.

Once a path has been found, the corresponding manipulation sequence can be executed: starting from the configuration i, each edge (s, s') in the path allows us to move the object from s to s' by opening the jaws and retracting the pins associated with s, then lowering the pins associated with s' and closing the jaws.

The grasp planning algorithm of Section 2 can of course be used to implement Step (1) of the algorithm. Finding "all" immobilizing configurations has, however, slightly different meanings in manipulation and grasping tasks, as explained in Section 3.2.1 below. As shown in Section 3.2.2, deciding whether an immobilizing configuration s belongs to the maximum ICS region of another configuration s' does not require an explicit boundary representation of ICS(s'). Indeed, the construction of G in Step (3) of our algorithm can be implemented efficiently by mapping it onto a *three-dimensional dominance* problem [39], as explained in Section 3.2.3. Finally, Step (4) can be implemented as a breadth-first search of the graph G. The overall complexity of the manipulation planning algorithm is analyzed in Section 3.2.4, and empirical results are presented in Section 3.3.

3.2.1   Triples of Pins: Prototypes and Shifts

As remarked earlier, the algorithm of Section 2 can be used to construct the immobilizing object/gripper configurations. There is however a difference between grasping and manipulation applications: during grasp planning, one can always assume that the first pin is at the origin with zero height. Of course, when a grasp is actually executed, the pin positions and heights, along with the jaw separation, all have to be shifted so that the corresponding variables are all positive and the pin positions remain within the extent of the top plate. Nonetheless, gripper configurations

that only differ by a shift of the three pin positions are equivalent for grasping purposes. This is not the case for in-hand manipulation, where the goal is to move the object held by the gripper across the bottom plate: this forces us to take into account all shifted configurations of a grasp.

We will say that a triple of pin positions with the first pin located at the origin is a *prototype*, and that all positions of the triple within the bottom plate are the *shifts* of this prototype. For each prototype, we can define the minimum rectangle aligned with the (p, q) coordinate axes and enclosing the pins. If W and H denote the width and height of this rectangle, and K^2 is the total number of grid elements, the prototype admits $(K - W)(K - H)$ different shifts, which can trivially be computed in time proportional to their number. According to Section 2.2.4, there are $O(D^2 d^2)$ immobilizing prototypes, to which correspond $O(D^2 d^4 K^2)$ shifted object/gripper configurations. If we assume that the manipulated object fits completely on the gripper's bottom plate, note that we will have $d \leq D \leq K$.

3.2.2 Testing whether a Configuration Belongs to the Maximum ICS Region of another Configuration

Constructing the graph G requires the ability to decide whether an immobilizing configuration s_a lies in the region ICS(s_b) associated with another configuration s_b. Let θ_a denote the orientation of the configuration s_a, and δ_b^* denote the critical jaw separation associated with s_b. A necessary condition for s_a to belong to ICS(s_b) is of course that s_a belongs to the range of orientations associated with δ_b^*.

When this necessary condition is fulfilled, let $T(\delta_b^*, \theta_a)$ denote the slice of ICS(s_b) at $\theta = \theta_a$. Then s_a will belong to ICS(s_b) if and only if s_a is inside $T(\delta_b^*, \theta_a)$. Note that constructing $T(\delta_b^*, \theta_a)$ does *not* require constructing an explicit boundary representation of ICS(s_b) then intersecting it with the plane $\theta = \theta_a$: instead, we construct the triangle directly from the lines $L_i(\delta_b^*, \theta_a)$ as explained in Section 3.1.1.

Thus constructing the graph only requires the ability of computing δ^* and the corresponding range or orientations, constructing the triangles $T(\delta^*, \theta)$ for discrete values of θ, and testing whether a point belongs to one of these triangles. Each one of these computations can be done in constant time.

3.2.3 Constructing the Graph

From Section 2, we know that for a given triple of pins, all immobilizing configurations of a given object will have the same orientation, independent of the pin heights. Of course, the immobilized orientation of the object remains the same when the triple of pins is arbitrarily shifted on the grid. Thus we can associate to each immobilizing prototype a plane $\theta =$ constant of the object's configuration space, and all the corresponding immobilizing configurations will lie in that plane. In other words, the vertices of the graph G will form layers of immobilized configurations (Figure 13(a)) corresponding to as many prototypes.

We now give an efficient algorithm for constructing the edges of the graph G. Let S_a and S_b be the sets of immobilized configurations corresponding to the layers $\theta = \theta_a$ and $\theta = \theta_b$ of the configuration space. We want to find all pairs of configurations s_a in S_a and s_b in S_b such that s_a lies within ICS(s_b) or equivalently within $T(\delta_b^*, \theta_a)$. This can of course be achieved by testing for each point-triangle pair whether the point belongs to the corresponding triangle. Instead, we observe that, following Section 3.1.1, the triangles $T(\delta_b^*, \theta_a)$ associated with all the elements of S_b are homothetic and, since θ is fixed, they also have the same orientation. This allows us to derive a more efficient method.
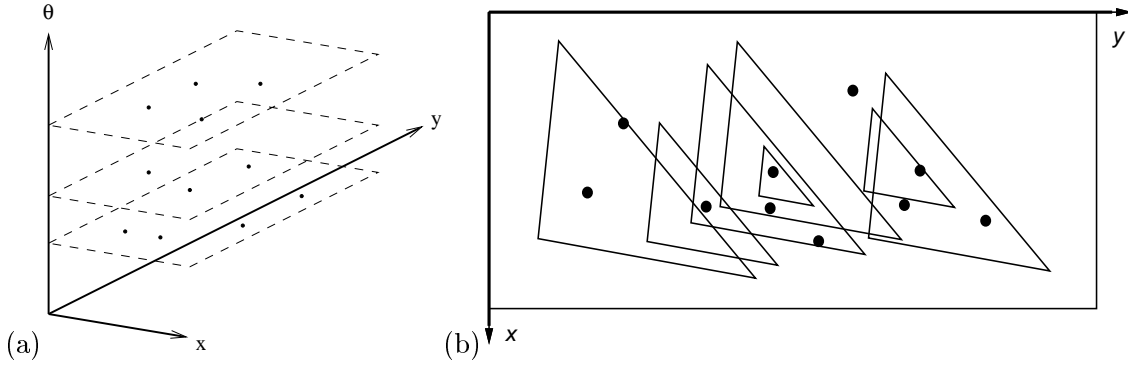
Figure 13: (a) layers of immobilized configurations of the object; (b) points and triangles within the same layer.

Let us restate the problem: given a set of points $P = \{p_1, p_2, .., p_n\}$, and a set $T = \{t_1, t_2, .., t_m\}$ of homothetic triangles having the same orientation, find all pairs (p_i, t_j) $(i = 1, .., n,\ j = 1, .., m)$ such that the point p_i is inside the triangle t_j (Figure 13(b)). This type of query is common in computational geometry: for example, Chazelle gave an optimal $O(\log m + r)$ algorithm for the related problem of finding the subset of m isothetic rectangles which contain a query point, where r is the number of rectangles returned [7].

This problem can be mapped onto another classical one through the following transformation: let $\boldsymbol{u}_i$ $(i = 1, 2, 3)$ denote the inward unit normals to the edges of the triangles. Given some choice of origin in the plane, we can associate with any point p its coordinates (x_1, x_2, x_3) along the vectors $\boldsymbol{u}_i$ (Figure 14). Likewise, we can associate with each triangle t the signed distances (y_1, y_2, y_3) between the origin and its edges along the vectors $\boldsymbol{u}_i$. Obviously p is inside t if and only if $x_i \geq y_i$ for $i = 1, 2, 3$. If we define the partial order $\succ$ over $\mathbb{R}^3$ by $(x_1, x_2, x_3) \succ (y_1, y_2, y_3)$ if and only if $x_i \geq y_i$ for $i = 1, 2, 3$, we have reduced our initial problem to the problem of finding the pairs of points p_i' in P' and t_j' in T' such that $p_i' \succ t_j'$, where P' and T' are subsets of $\mathbb{R}^3$ containing respectively n and m points. This is the problem called "3D Merge Dominance" by Preparata and Shamos [39, pp. 357–363], who give a simple divide-and-conquer algorithm for solving this problem in $O((m + n)\log(m + n) + s)$ time and $O(m + n)$ space, where s is the number of pairs found by the algorithm.
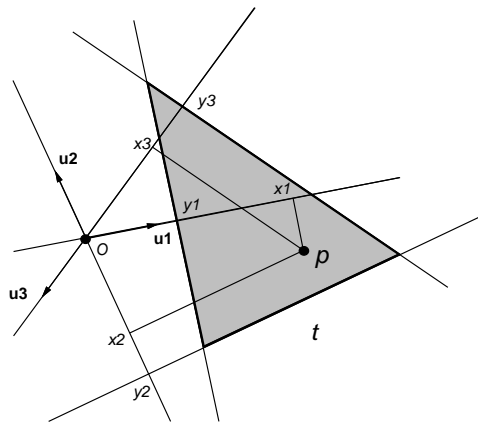
Figure 14: Three-dimensional coordinates associated with a point p and a triangle t.

3.2.4 Algorithm Analysis

The cost of the algorithm is dominated by the construction of the graph. Let V denote the number of immobilizing gripper configurations (or equivalently the number of vertices of G), and let P denote the number of prototypes associated with these configurations. Note that $P = O(D^2 d^2)$ and $V = O(P d^2 K^2)$ according to the analysis of Section 2. Let E denote the number of edges of G. Since each prototype yields $O(d^2 K^2)$ shifted configurations and $d \leq K$, it follows from the analysis of the dominance algorithm that the construction of the graph takes $O(P^2 d^2 K^2 \log K + V + E)$ time. Of course, $E = O(V^2)$.

3.3 Implementation and Results

We have implemented the manipulation planning algorithm, including its 3D dominance part, and tested our implementation using a 5×5 grid resolution. As before, the program has been written in C, and all run times have been measured on a SUN SPARCstation 10.

Figure 15 shows an example of maximum ICS region in the configuration space (x, y, θ) for one of the immobilized configurations of a tetrahedron. Note that this graphical representation is for display only: our algorithm does not construct an explicit boundary representation of the ICS. Instead, we compute the corresponding δ^* value and the associated range of orientations. Our grasp planning program finds 208 prototypes and 33,868 shifted immobilizing configurations, and the corresponding ICS computation takes 13 seconds. The graph G contains 1,247,374 edges, and its construction takes 156 seconds.

(a)   (b)   (c)
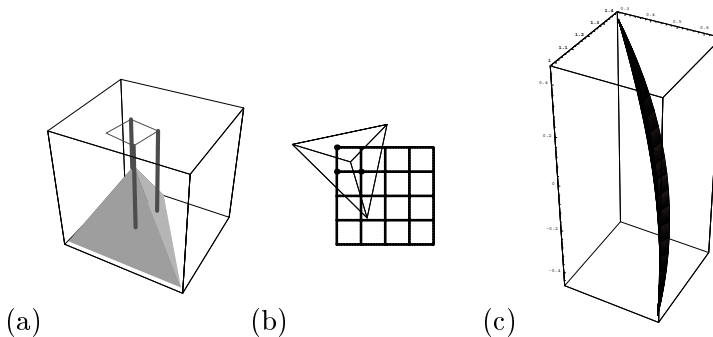
Figure 15: An ICS region in configuration space: (a)-(b) two views of an immobilized configuration of a tetrahedron; (c) the corresponding ICS region.

Once the graph has been constructed, the search for sequences of gripper configurations is quite efficient: a simple breadth-first approach has been used in our experiments to search the graph G, and the search time is below 1 second in all cases.

Figures 16 and 17 show two examples. In the first one, the program finds a 4-step sequence to move the object from the configuration shown in Figure 16(a) to the one shown in Figure 16(b). Note that, although the pin configurations are the same in Figures 16(c) and 16(d), the pin lengths are actually different, yielding different object positions.

Figure 17 shows a more complicated example, where the program finds a 72-step sequence of gripper configurations to move the object from the configuration shown in Figure 17(a) to the one shown in Figure 17(b).
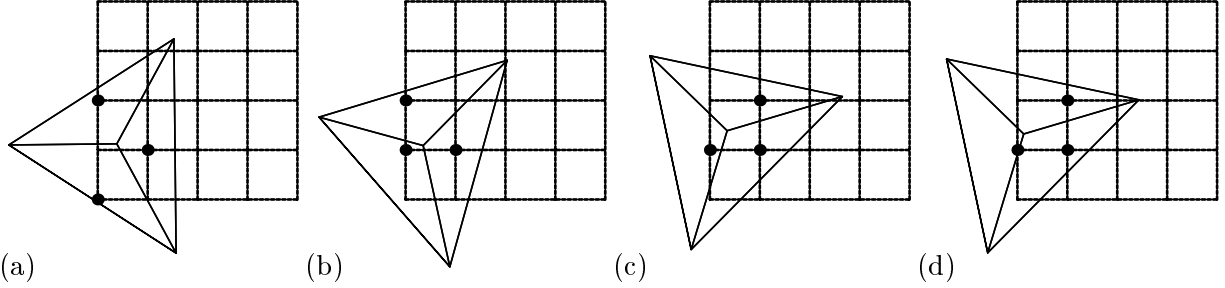
Figure 16: The four steps of a manipulation sequence for moving a tetrahedron from configuration (a) to configuration (d).
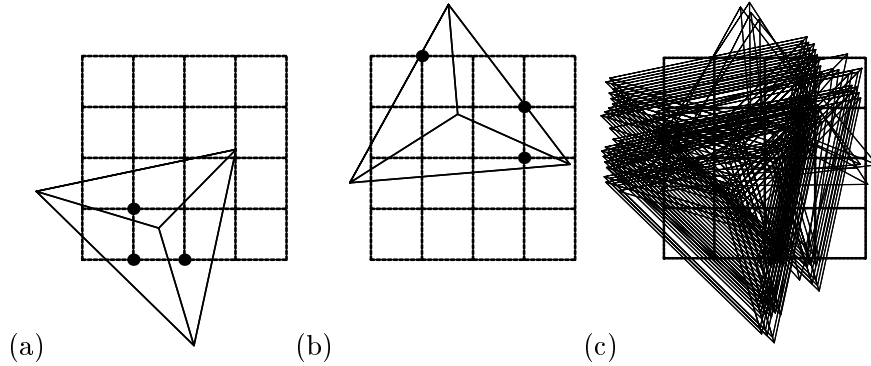
Figure 17: Another example: (a) initial configuration, (b) goal configuration, (c) sequence of moves.

4   Discussion

As noted in the Introduction, we are currently in the process of constructing the reconfigurable gripper: the mechanical design and assembly are complete, and we are completing the electronics and computer interface for the control unit. Thus we hope to be able to report experimental results using the actual gripper within a few weeks.

We are investigating a number of extensions of the work presented in this paper. First, the grasp planning algorithm generalizes to fixture planning, and Figure 18 shows a three-dimensional fixture synthesized by the algorithm of [35, 49]. We are also looking at grasp and fixture planning for devices that have a variety of discrete and continuous degrees of freedom, for example fixtures using rotating clamps.

We are also investigating various extensions of our in-hand manipulation approach: for example, the stepper motors used to actuate the pins of our reconfigurable gripper allow essentially continuous vertical motions of the pins. We plan to address the problem of constructing manipulation plans that exploit these continuous degrees of freedom.

Finally, although the algorithms presented in this paper have proven efficient in our experiments, it would be interesting to establish the intrinsic complexity of the grasp and manipulation planning problems, and of course to develop optimal algorithms achieving this complexity.
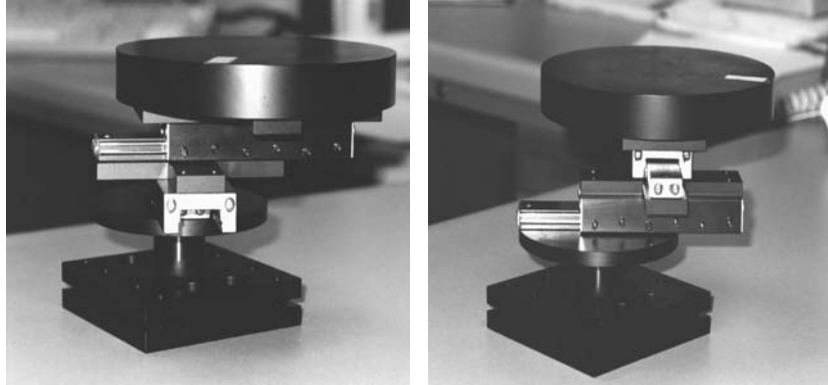
Figure 18: Three-dimensional fixtures.

References

[1] S. Akella and M.T. Mason. Parts orienting by push-aligning. In *IEEE Int. Conf. on Robotics and Automation*, pages 414–420, Nagoya, Japan, May 1995.

[2] R.S. Ball. *A treatise on the theory of screws*. Cambridge University Press, 1900.

[3] A. Blake. Computational modelling of hand-eye coordination. *Phil. Trans. R. Soc. Lond. B*, 337:351–360, 1992.

[4] R.C. Brost and K. Goldberg. A complete algorithm for synthesizing modular fixtures for polygonal parts. In *IEEE Int. Conf. on Robotics and Automation*, pages 535–542, San Diego, CA, May 1994.

[5] R.C. Brost and R.R. Peters. Automatic design of 3D fixtures and assembly pallets. In *IEEE Int. Conf. on Robotics and Automation*, pages 495–502, Minneapolis, MN, April 1996.

[6] J.F. Canny and K.Y. Goldberg. "RISC" for industrial robotics: recent results and open problems. In *IEEE Int. Conf. on Robotics and Automation*, pages 1951–1958, San Diego, CA, 1994.

[7] B.M. Chazelle. Filtering search: a new approach to query answering. In *IEEE Symposium on Foundatons of Computer Science*, pages 122–132, Tucson, AZ, November 1983.

[8] I.M. Chen and J.W. Burdick. Finding antipodal point grasps on irregularly shaped objects. In *IEEE Int. Conf. on Robotics and Automation*, pages 2278–2283, Nice, France, June 1992.

[9] Y.C. Chou, V. Chandru, and M. Barash. A mathematical approach to automatic configuration of machining fixtures: analysis and synthesis. *ASME Journal of Engineering for Industry*, 111:299–306, 1989.

[10] J. Czyzowicz, I. Stojmenovic, and J. Urrutia. Immobilizing a polytope. volume 519 of *Lecture Notes in Computer Sciences*, pages 214–227. Springer-Verlag, 1991.

[11] J. Donoghue, W.S. Howard, and V. Kumar. Stable workpiece fixturing. In 23rd *biennial ASME mechanics conference*, Minneapolis, Sept. 1994.

[12] M.A. Erdmann and M.T. Mason. An exploration of sensorless manipulation. *IEEE Journal of Robotics and Automation*, 4:369–379, 1988.

[13] C. Ferrari and J.F. Canny. Planning optimal grasps. In *IEEE Int. Conf. on Robotics and Automation*, pages 2290–2295, Nice, France, June 1992.

[14] J.B.J. Fourier. Reported in: Analyse des travaux de l'académie royale des sciences pendant l'année 1824. In *Partie mathématique, Histoire de l'Académie Royale des Sciences de l'Institut de France*, volume 7, xlvii-lv. 1827. Partial English translation in: D.A. Kohler, Translation of a Report by Fourier on his work on Linear Inequalities, *Opsearch* 10 (1973) 38-42.

[15] K.Y. Goldberg. A kinematically-yielding gripper. In 22nd *Int. Symp. on Industrial Automation*, 1992. See U.S. Patent 5,098,145.

[16] K.Y. Goldberg. Orienting polygonal parts without sensors. *Algorithmica*, 10(2):201–225, 1993.

[17] W.S. Howard and V. Kumar. Stability of planar grasps. In *Proc. IEEE Int. Conf. on Robotics and Automation*, pages 2822–2827, San Diego, CA, May 1994.

[18] K.H. Hunt. *Kinematic Geometry of Mechanisms*. Clarendon, Oxford, 1978.

[19] S.C. Jacobsen, J.E. Wood, D.F. Knutti, and K.B. Biggers. The Utah-MIT Dextrous Hand: Work in progress. *International Journal of Robotics Research*, 3(4):21–50, 1984.

[20] K. Lakshminarayana. Mechanics of form closure. Technical Report 78-DET-32, ASME, 1978.

[21] C. Lassez and J-L. Lassez. Quantifier elimination for conjunctions of linear constraints via a convex hull algorithm. In B. Donald, D. Kapur, and J. Mundy, editors, *Symbolic and Numerical Computation for Artificial Intelligence*, pages 103–122. Academic Press, 1992.

[22] J-L. Lassez. Querying constraints. In *ACM conference on Principles of Database Systems*, Nashville, 1990.

[23] S.H. Lee and M.R. Cutkosky. Fixture planning with friction. *Trans. of the ASME*, 112:320–327, August 1991.

[24] K.M. Lynch and M.T. Mason. Stable pushing: mechanics, controllability, and planning. In K.Y. Goldberg, D. Halperin, J.-C. Latombe, and R. Wilson, editors, *Algorithmic Foundations of Robotics*, pages 239–262. A.K. Peters, 1995.

[25] X. Markenscoff and C.H. Papadimitriou. Optimum grip of a polygon. *International Journal of Robotics Research*, 8(2):17–29, April 1989.

[26] M.T. Mason. Mechanics and planning of manipulator pushing operations. *International Journal of Robotics Research*, 5(3):53–71, 1986.

[27] B. Mirtich and J.F. Canny. Optimum force-closure grasps. Technical Report ESRC 93-11/RAMP 93-5, Robotics, Automation, and Manufacturing Program, University of California at Berkeley, July 1993.

[28] B. Mishra. Worksholding – analysis and planning. In *IEEE/RSJ Int. Workshop on Intelligent Robots and Systems*, pages 53–56, Osaka, Japan, 1991.

[29] B. Mishra, J.T. Schwartz, and M. Sharir. On the existence and synthesis of multifinger positive grips. *Algorithmica, Special Issue: Robotics*, 2(4):541–558, November 1987.

[30] B. Mishra and N. Silver. Some discussion of static gripping and its stability. *IEEE Systems, Man, and Cybernetics*, 19(4):783–796, 1989.

[31] V-D. Nguyen. Constructing force-closure grasps. *International Journal of Robotics Research*, 7(3):3–16, June 1988.

[32] V-D. Nguyen. Constructing stable grasps. *International Journal of Robotics Research*, 8(1):27–37, February 1989.

[33] M.S. Ohwovoriole. An extension of screw theory. *Journal of Mechanical Design*, 103:725–735, 1981.

[34] N.S. Pollard and T. Lozano-Pérez. Grasp stability and feasibility for an arm with an articulated hand. In *IEEE Int. Conf. on Robotics and Automation*, pages 1581–1585, Cincinatti, OH, 1990.

[35] J. Ponce. On planning immobilizing fixtures for three-dimensional polyhedral objects. In *IEEE Int. Conf. on Robotics and Automation*, pages 509–514, Minneapolis, MN, April 1996.

[36] J. Ponce and B. Faverjon. On computing three-finger force-closure grasps of polygonal objects. *IEEE Transactions on Robotics and Automation*, 11(6):868–881, December 1995.

[37] J. Ponce, D. Stam, and B. Faverjon. On computing force-closure grasps of curved two-dimensional objects. *International Journal of Robotics Research*, 12(3):263–273, June 1993.

[38] J. Ponce, S. Sullivan, A. Sudsang, J-D. Boissonnat, and J-P. Merlet. On computing four-finger equilibrium and force-closure grasps of polyhedral objects. *International Journal of Robotics Research*, 16(1):11–35, February 1997.

[39] F.P. Preparata and M.I. Shamos. *Computational Geometry - An Introduction*. Springer-Verlag, 1985.

[40] A.S. Rao and K.Y. Goldberg. Manipulating algebraic parts in the plane. *IEEE Transactions on Robotics and Automation*, pages 598–602, 1995.

[41] F. Reulaux. *The kinematics of machinery*. MacMillan, NY, 1876. Reprint, Dover, NY, 1963.

[42] E. Rimon and A. Blake. Caging 2D bodies by one-parameter two-fingered gripping systems. In *IEEE Int. Conf. on Robotics and Automation*, pages 1458–1464, Minneapolis, MN, April 1996.

[43] E. Rimon and J. W. Burdick. Towards planning with force constraints: On the mobility of bodies in contact. In *Proc. IEEE Int. Conf. on Robotics and Automation*, pages 994–1000, Atlanta, GA, May 1993.

[44] E. Rimon and J. W. Burdick. Mobility of bodies in contact-I: A new 2nd order mobility index for multi-finger grasps. *IEEE Transactions on Robotics and Automation*, 1995. Submitted. A preliminary version appeared in *IEEE Int. Conf. on Robotics and Automation*, pages 2329-2335, San Diego, CA, 1994.

[45] E. Rimon and J. W. Burdick. Mobility of bodies in contact-II: How forces are generated by curvature effects? *IEEE Transactions on Robotics and Automation*, 1995. Submitted. A preliminary version appeared in *IEEE Int. Conf. on Robotics and Automation*, pages 2336-2341, San Diego, CA, 1994.

[46] B. Roth. Screws, motors, and wrenches that cannot be bought in a hardware store. In *Int. Symp. on Robotics Research*, pages 679–693. MIT Press, 1984.

[47] J.K. Salisbury. *Kinematic and force analysis of articulated hands*. PhD thesis, Stanford University, Stanford, CA, 1982.

[48] P. Somov. Über Gebiete von Schraubengeschwindigkeiten eines starren Korpers bie verschiedener Zahl von Stutzflachen. *Zeitricht für Mathematik und Physik*, 45:245–306, 1900.

[49] A. Sudsang, J. Ponce, and N. Srinivasa. Algorithms for constructing immobilizing fixtures and grasps of three-dimensional objects. In J.-P. Laumont and M. Overmars, editors, *Algorithmic Foundations of Robotics II*, pages 363–380. AK Peters, Ltd., 1997.

[50] R. Wagner, Y. Zhuang, and K. Goldberg. Fixturing faceted parts with seven modular struts. In *IEEE Int. Symp. on Assembly and Task Planning*, pages 133–139, Pittsburgh, PA, August 1995.

[51] A. Wallack and J.F. Canny. Planning for modular and hybrid fixtures. In *IEEE Int. Conf. on Robotics and Automation*, pages 520–527, San Diego, CA, 1994.

[52] A.S. Wallack. *Algorithms and Techniques for Manufacturing*. PhD thesis, Computer Science Division, Univ. of California at Berkeley, 1995.

[53] Y. Zhuang, K. Goldberg, and Y.C. Wong. On the existence of modular fixtures. In *IEEE Int. Conf. on Robotics and Automation*, pages 543–549, San Diego, CA, May 1994.